SUPPLEMENTAL DATA

Paracrine Apoptotic Effect of p53 Mediated by Tumor Suppressor Par-4

Ravshan Burikhanov, Tripti Shrestha-Bhattarai, Nikhil Hebbar, Shirley Qiu,
Yanming Zhao, Gerard P. Zambetti, and Vivek M. Rangnekar

FIGURE S1

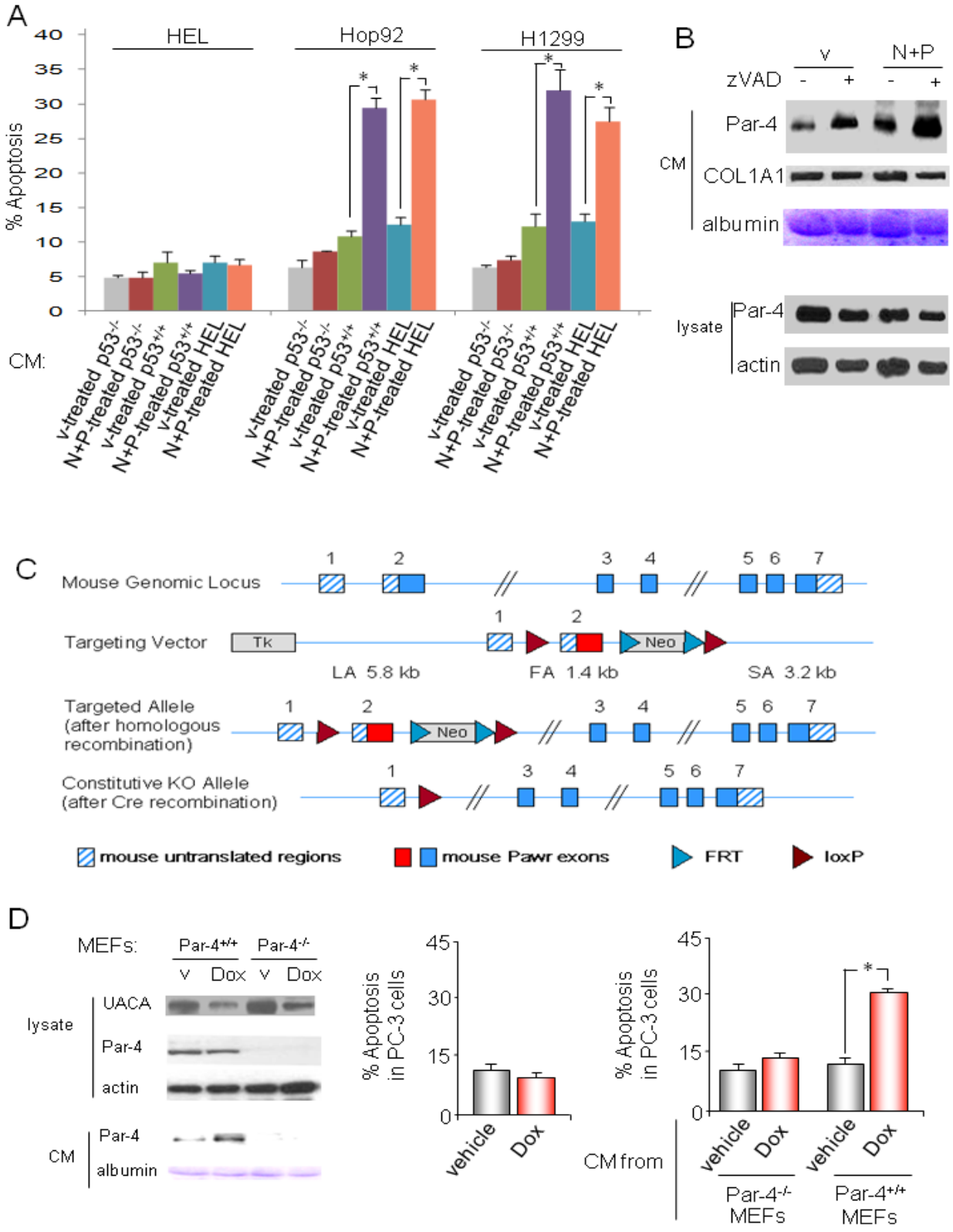

SUPPLEMENTAL DATA

Figure S1 Related to Figure 1. Par-4 in the CM is responsible for mediating the paracrine apoptotic effect of p53 in p53-deficient cancer cells.

(A) Sensitivity of various cells lines to the paracrine apoptotic effect of p53 activation in normal cells. Nutlin-3a belongs to a class of *cis*-imidazoline derivatives that selectively disrupt the interaction between p53 and MDM2 (Vassilev et al., 2004). The release of p53 from negative control by MDM2 results in direct activation of the p53 pathway, avoiding the nonspecific genotoxic damage inflicted by many classic cytotoxic drugs and radiation. Nutlin-3a induces growth arrest and cell death in cancer cells expressing functional p53, but is not directly effective in p53-mutant cancer cells; and it induces only reversible growth arrest in normal cells (Cheok et al., 2007; Kranz and Dobbelstein, 2006). To study the effect of p53 activation on paracrine apoptosis, we used Nutlin-3a alone or combined Nutlin-3a with PS-1145, a small molecule that specifically inhibits IKKβ (Hideshima et al., 2002). $P53^{+/+}$ or $p53^{-/-}$ MEFs and HEL cells were treated with vehicle (v), Nutlin-3a (N, 10 μM) and/or PS-1145 (P, 10 μM) for 24 h and the CM was transferred to various normal (HEL) and p53-deficient cancer (H1299, HOP-92) cell lines. After 24 h, the cells were scored for apoptosis.

(B) Par-4 secretion in response to p53 activation does not require apoptosis of the normal cells. $P53^{+/+}$ MEFs were treated with z-VAD-fmk (2 μM) and with Nutlin-3a (N, 10 μM) plus PS-1145 (P, 10 μM) or vehicle (v) for 24 h. The CM was examined for Par-4 levels by Western blot analysis.

(C) Generation of Par-4/Pawr knock out mice. Par-4 knock out (KO) mice were generated using the C57BL/6 mouse background. As Exon 2 contains the initiating ATG codon, it was flanked by loxP sites. The selection marker (Neomycin, Neo) was flanked by FRT sites and introduced into intron 2. Constitutive knock out allele was generated after *in vivo* Cre-mediated recombination that resulted in deletion of Exon 2 and loss of Par-4 function, owing to removal of the initiating ATG codon. $Par\text{-}4^{+/-}$ mice were intercrossed to generate $Par\text{-}4^{-/-}$ mice. Par-4 null mice grow normally and develop spontaneous tumors in diverse tissues as previously reported (Moreno-Bueno et al., 2007). MEFs isolated from the $Par\text{-}4^{-/-}$ mice and corresponding $Par\text{-}4^{+/+}$ littermate control mice were studied for Par-4 secretion.

(D) Doxorubicin induces paracrine apoptosis of cancer cells by Par-4 secretion. PC-3 cells were treated with 100 nM doxorubicin (Dox) or vehicle for 24 h and scored for apoptosis by ICC for active caspase-3 (middle panel). Note 100 nM Dox does not directly induce apoptosis in PC-3 cells. $Par\text{-}4^{+/+}$ or $Par\text{-}4^{-/-}$ MEFs were treated with 100 nM doxorubicin (Dox) or vehicle for 24 h and the CM from these cells was transferred to PC-3 cells; after 24 h the PC-3 cells were scored for apoptosis (right panel). Elevation of Par-4 in the CM of doxorubicin (Dox)- or vehicle (v)-treated $Par\text{-}4^{+/+}$ or $Par\text{-}4^{-/-}$ MEFs was confirmed by Western blot analysis (left panel).

SUPPLEMENTAL DATA

FIGURE S2

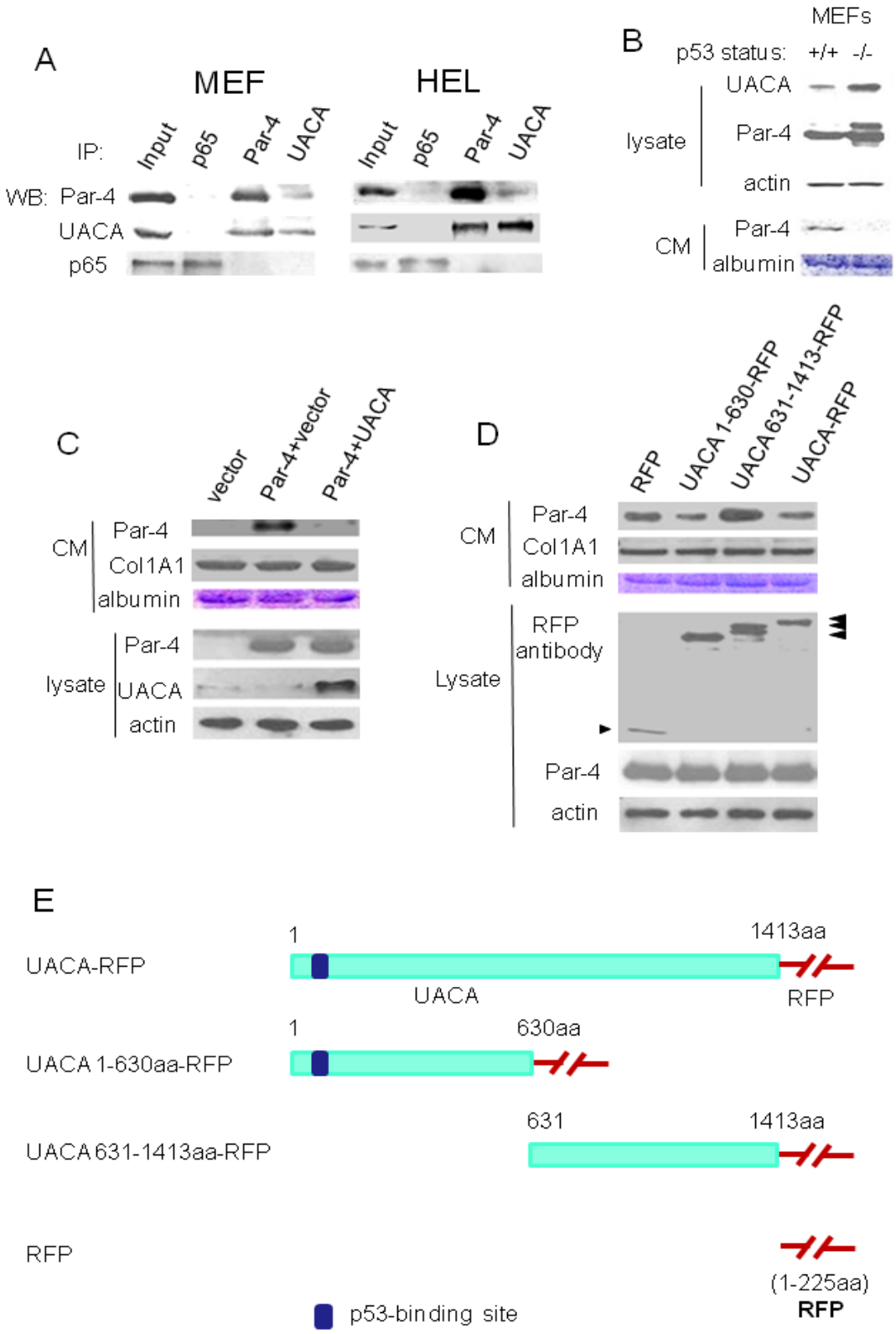

SUPPLEMENTAL DATA

Figure S2 Related to Figure 3. UACA binds to Par-4 to inhibit Par-4 secretion, and p53 down-regulates UACA to restore Par-4 secretion.

(A) UACA binds to Par-4 in fibroblasts. Whole-cell lysates of human lung fibroblasts HEL and $p53^{+/+}$ MEFs were subjected to co-immunoprecipitation with Par-4, UACA, or p65/NF-κB (control) antibody. The immunoprecipitates and input lysates were examined by Western blot analysis. Similar to our findings in epithelial cells (Burikhanov et al., 2013), UACA binds to Par-4 in fibroblasts.

(B) UACA down-regulation by p53 correlates with Par-4 secretion. CM or whole-cell lysates from $p53^{+/+}$ and $p53^{-/-}$ MEFs were subjected to Western blot analysis for UACA or Par-4 expression. Note UACA is down-regulated in $p53^{+/+}$ cells. Consistently, *UACA*-null mice grow normally and do not exhibit significant phenotypes (Kiso et al., 2012; Sakai et al., 2010), indicating that UACA function is dispensable for survival of normal cells.

(C) Ectopic expression of UACA inhibits the secretion of Par-4. MEFs from $Par\text{-}4^{-/-}$ mice were co-transfected with Par-4 expression construct plus vector control, Par-4 and UACA expression construct (1:1 ratio), or with vector control. Transfected populations were selected, confirmed for stable expression of Par-4 and UACA using whole-cell lysates, and then secretion of Par-4 in the CM was examined by Western blot analysis.

(D) UACA binding to Par-4 is essential in order to prevent Par-4 secretion. $Par\text{-}4^{+/+}$ MEF cells were transfected with expression constructs for Red Fluorescent Protein (RFP; vector), RFP-tagged UACA, or RFP-tagged UACA deletion mutants, 1-630 (which binds to Par-4) or 631-1413 (which does not bind to Par-4) (Burikhanov et al., 2013). Transfected populations were selected, confirmed for stable expression of UACA or UACA-mutants using whole-cell lysates, and secretion of Par-4 in their CM was determined by Western blot analysis.

(E) Illustration of full length UACA and deletion mutants of UACA subcloned in the CMV-promoter based expression vector pCB6. Full length UACA or deletion mutants 1-630aa or 631-1413aa (with in-frame RFP tagged at its C-terminus) are shown. The sizes of full-length UACA and mutant UACA fragments subcloned into pDsRed vector are indicated.

SUPPLEMENTAL DATA

FIGURE S3

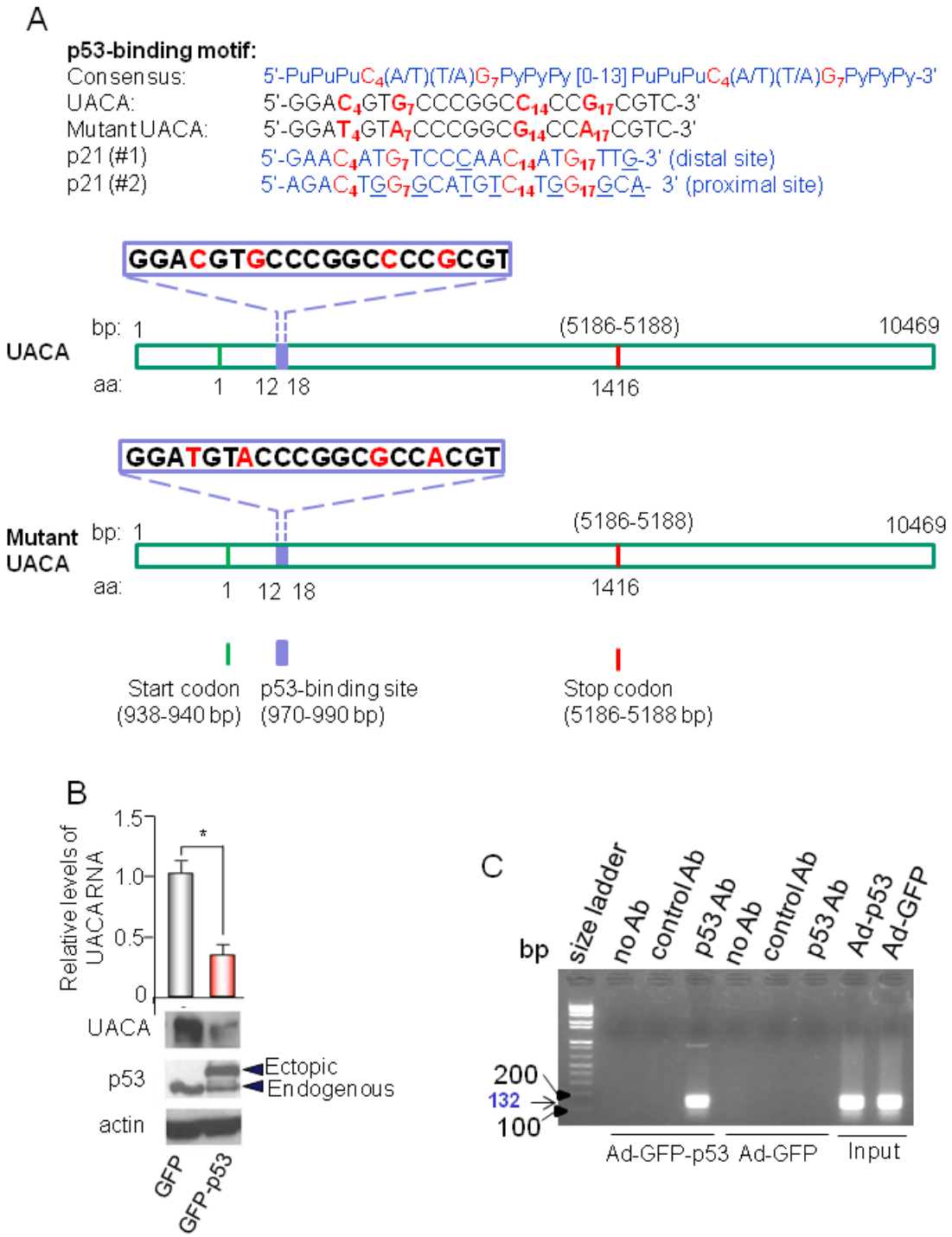

SUPPLEMENTAL DATA

Figure S3 Related to Figures 3 and 4. *UACA* contains a p53 consensus binding motif and p53 down-regulates *UACA* by directly binding to *UACA* DNA.

(A) Comparison of the p53 response elements in UACA and p21, and location of wild type p53 binding motif and mutations introduced in UACA. The consensus sequence for p53-binding DNA motif is shown along with the p53-binding motifs in UACA and p21. The indicated mutations were introduced at C4, G7, C14 and G17 into the p53-binding motif of UACA. P21 has two p53-binding motifs (#1 and #2) (El-Deiry et al., 1995). The nucleotides in the p53-binding motif of p21 that deviate from the p53 consensus binding motif are underlined. Mutant-UACA with the altered p53-binding site was generated by PCR using mutant-UACA primers and wild type UACA DNA as template, and fidelity of the UACA constructs was confirmed by Retrogen Inc., CA.

(B) P53 inhibits the expression of UACA RNA. Cells were infected with either control GFP-producing adenovirus or GFP-tagged p53-producing adenovirus for 24 h. Total RNA was isolated from each of the samples and subjected to qRT-PCR (upper panel), or whole cell lysates were subjected to Western blot analysis (lower panel).

(C) P53 binds to its consensus binding motif in *UACA*. A putative p53 binding motif (5'-GGA**C_4**GT**G_7**CCCGGC**C_{14}**CC**G_{17}**CGTC-3'; where C4 and G7 have been previously shown to be critical) (El-Deiry et al., 1992) is present in the coding region of UACA. P53-deficient cells were infected with GFP-tagged p53- or GFP-producing adenovirus and subjected to ChIP analysis with p53 antibody (Ab) or control rabbit Ab, and immunoprecipitated DNA fragments were analyzed by PCR with primers flanking the p53 binding site.

SUPPLEMENTAL DATA

FIGURE S4

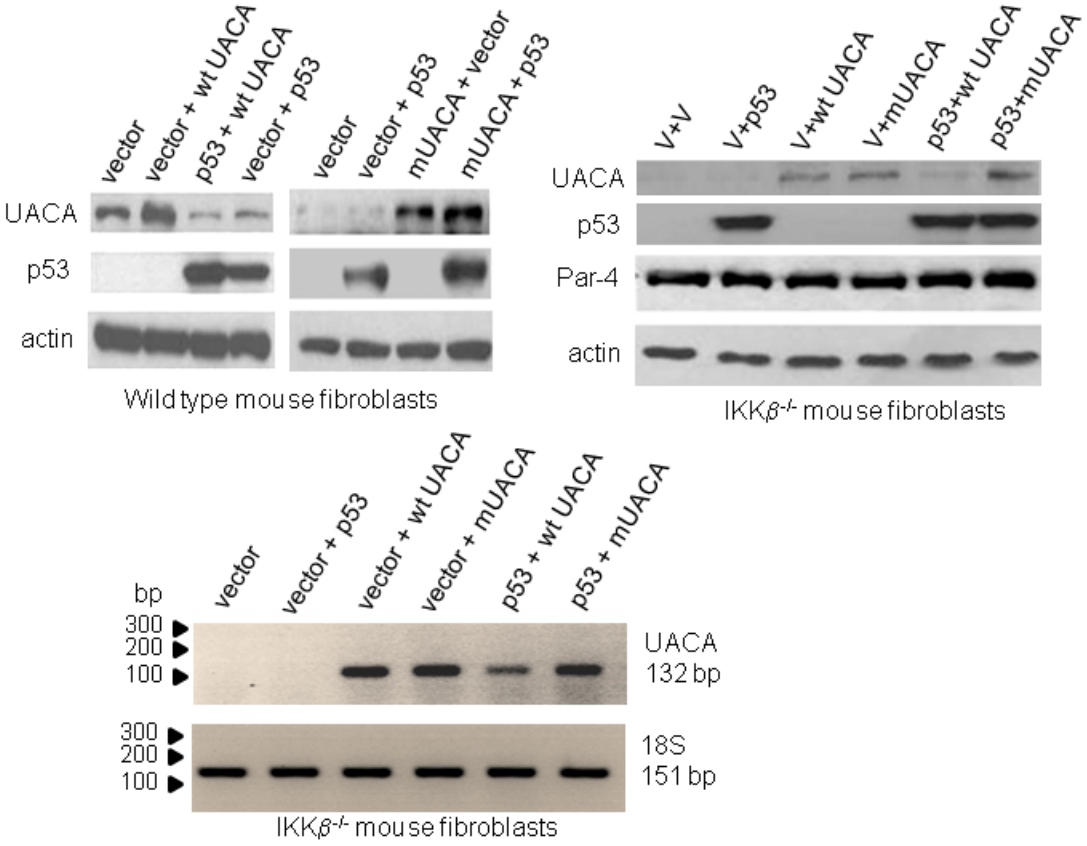

Figure S4 Related to Figure 4. P53 regulates UACA expression via its binding motif in an NF-κB activity-independent manner. IKKβ$^{-/-}$ MEFs (right and bottom panels) or wild type MEFs (left panel), as controls, were co-transfected with the indicated expression constructs. Whole-cell lysates were subjected to Western blot analysis for UACA, p53 or actin (top panels) or RNA was prepared from the cells and subjected to reverse transcriptase PCR for UACA and 18S rRNA (bottom panel). Wild type (wt) UACA contained wild type p53-binding motif 5'-GGA**C$_4$**GT**G$_7$**CCCGGC**C$_{14}$**C C**G$_{17}$**CGTC-3', and mutant (m) UACA contained mutations 5'-GGA**T$_4$**GT**A$_7$**CCCGGC**G$_{14}$**CC**A$_{17}$**CGTC-3' in the p53 binding sequence.

SUPPLEMENTAL DATA

SUPPLEMENTAL EXPERIMENTAL PROCEDURES

Plasmids and chemical reagents

z-VAD-fmk was from BioVision, and PS-1145, Doxorubicin and BFA were from Sigma Chemicals. UACA-constructs were described previously (Burikhanov et al., 2013). The p53 constructs were from Wafik El-Deiry (Penn State University, PA). Transfections were performed using Lipofectamine and Plus reagents (Invitrogen).

Antibodies and siRNA duplexes

The polyclonal antibodies for UACA were from Bethyl Laboratories and Abcam. Par-4 (R332), Col1A1 (H-197), pan-cytokeratin (C11), p53 (FL-393), p21/WAF1 (F5), PTEN (FL-403) and rabbit IgG antibodies were from Santa Cruz Biotechnology, Inc. The mouse monoclonal antibody for p53 (1C12 mAb), and cleaved caspase-3 antibody (D175) were from Cell Signaling, and that for β-actin was from Sigma Chemical Corp. The control siRNA and pools of siRNA for UACA were from Dharmacon and SantaCruz Biotechnology, Inc.

Co-immunoprecipitation and Western blot analysis

Protein extracted from cell lysates was filtered, pre-cleared with 25 µl (bed volume) of protein G-Sepharose beads and immunoprecipitated with 1 µg of respective antibodies. The eluted proteins were resolved by SDS-PAGE, and subjected to Western blot analysis as described (Goswami et al., 2008).

Quantitative Real Time-PCR analysis

Approximately $1x10^6$ cells were infected with GFP control or GFP-tagged p53-adenovirus for 24 hours, and total RNA was extracted using Trizol reagent. Quantitative Real Time-PCR (qRT-PCR) was performed using SuperScript First-Strand Synthesis System (Invitrogen) using oligo (dT) primers for RT. Brilliant II SYBR Green Master Mix (Agilent Technologies) was used for subsequent qPCR. Primers used were as follows: Forward: 5'-cgc cc tag agg tga aat tct-3' and reverse: 5'-cga acc tcc gac ttt cgt tct-3' for 18S RNA, and forward primer: 5'-ggc gga gaa cga taa gtt gac taa-3', and reverse primer: 5'-cat gtt tct cgg gag cta caa ac-3' for qPCR of human UACA.

Reverse transcriptase-PCR analysis

For the reverse-transcriptase PCR experiment with co-transfection, approximately $1.5x10^6$ IKKβ$^{-/-}$ cells were co-transfected with either vector, wild-type(wt) UACA, or mutant(m) UACA construct with or without p53 plasmid for 72 hours, and total RNA was extracted using RNeasy mini kit (Qiagen). Reverse transcription was performed to synthesize cDNA with random hexamers using SuperScript III First-Strand Synthesis System (Invitrogen), and was followed by PCR. Primers used were as follows:
Forward primer: 5'- gta acc cgt tga acc cca tt -3' and reverse primer: 5'- cca tcc aat cgg tag tag cg -3' for 18S RNA.
Forward primer: 5'-aag agc ctc aag tcc cgc c -3', and reverse primer: 5'- ccc ccc ttt ctg ctg ctt-3' for pCB6$^+$ human UACA wild type or mutant constructs. The products were subjected to DNA gel electrophoresis.

SUPPLEMENTAL DATA

ChIP analysis

ChIP assays for endogenous p53 binding to the consensus binding site in UACA were performed by treating $2x10^6$ HEL cells with either DMSO vehicle or with Nutlin-3a for 24 h, and $1x10^6$ cells were used per ChIP reaction in each treatment group. Alternatively, for ChIP analysis with ectopic p53 expression, $1x10^6$ cells infected with either GFP control or GFP-tagged p53-adenovirus were used per ChIP assay. ChIP analysis was performed using the ChIP kit from Millipore according to the instructions provided by the manufacturer. Briefly, the proteins and DNA were cross-linked with 1% formaldehyde, lysed, and the DNA was sheared into 200-800 bp fragments. Proteins linked to the DNA were immunoprecipitated with appropriate antibodies (using rabbit IgG or no antibody as control). Subsequently, immune complexes were eluted from the beads, protein-DNA crosslinks were reversed, and DNA was isolated after phenol/chloroform/isoamyl alcohol extraction followed by ethanol precipitation. DNA fragments were amplified by PCR using the following primers.

UACA: Forward primer 5'-gtc tac tcc ttg cgc gct gg-3' and reverse primer 5'-gcg gcg cca gac gac-3'.

p21: Forward primer 5'-ctg gac tgg gca ctc ttg tc- 3' and reverse primer 5'-ctc cta cca tcc cct tcc tc- 3'

GAPDH: Forward primer 5' – atg gtt gcc act ggg gat ct- 3' and reverse primer 5' – tgc caa agc cta ggg gaa ga- 3'

Apoptosis assays

Apoptotic nuclei were identified by immunocytochemical (ICC) analysis for active caspase-3, or by 4, 6-diamidino-2-phenylindole (DAPI) staining. A total of three independent experiments were performed; and approximately 500 cells were scored in each experiment for apoptosis under a fluorescent microscope.

SUPPLEMENTAL ACKNOWLEDGMENTS

The authors thank Sunil K. Noothi, Ph.D., University of Kentucky for thoughtful suggestions on the ChIP assays.

SUPPLEMENTAL REFERENCES

Cheok, C. F., Dey, A., and Lane, D. P. (2007). Cyclin-dependent kinase inhibitors sensitize tumor cells to nutlin-induced apoptosis: a potent drug combination. Mol Cancer Res *5*, 1133-1145.

El-Deiry, W.S., Tokino, T., Waldman T, Oliner, J.D., Velculescu, V.E., Burrell, M., Hill, D.E., Healy, E., Rees, J.L., Hamilton S.R. et. al. (1995). Topological control of p21WAF1/CIP1 expression in normal and neoplastic tissues. Cancer Res 55, 2910-2919.

Goswami, A., Qiu, S., Dexheimer, T. S., Ranganathan, P., Burikhanov, R., Pommier, Y., and Rangnekar, V. M. (2008). Par-4 binds to topoisomerase 1 and attenuates its DNA relaxation activity. Cancer Res *68*, 6190-6198.

SUPPLEMENTAL DATA

Hideshima, T., Chauhan, D., Richardson, P., Mitsiades, C., Mitsiades, N., Hayashi, T., Munshi, N., Dang, L., Castro, A., Palombella, V*., et al.* (2002). NF-kappa B as a therapeutic target in multiple myeloma. J Biol Chem *277*, 16639-16647.

Kiso, K., Ueno, S., Fukuda, M., Ichi, I., Kobayashi, K., Sakai, T., Fukui, K., and Kojo, S. (2012). The role of Kupffer cells in carbon tetrachloride intoxication in mice. Biol Pharm Bull *35*, 980-983.

Kranz, D., and Dobbelstein, M. (2006). Nongenotoxic p53 activation protects cells against S-phase-specific chemotherapy. Cancer Res *66*, 10274-10280.

Moreno-Bueno**,** G**.**, Fernandez-Marcos**,** P**.**J**.**, Collado**,** M**.**, Tendero**,** M**.**J**.**, Rodriguez-Pinilla**,** S**.**M**.**, Garcia-Cao**,** I**.**, Hardisson**,** D**.**, Diaz-Meco**,** M**.**T**.**, Moscat**,** J**.**, Serrano**,** M**.**, and Palacios**,** J. (2007). Inactivation of the candidate tumor suppressor par-4 in endometrial cancer. Cancer Res *67*, 1927-1934.

Sakai, T., Liu, L., Teng, X., Ishimaru, N., Mukai-Sakai, R., Tran, N. H., Kim, S. M., Sano, N., Hayashi, Y., Kaji, R., and Fukui, K. (2010). Inflammatory disease and cancer with a decrease in Kupffer cell numbers in Nucling-knockout mice. Int J Cancer *126*, 1079-1094.

Vassilev, L. T., Vu, B. T., Graves, B., Carvajal, D., Podlaski, F., Filipovic, Z., Kong, N., Kammlott, U., Lukacs, C., Klein, C*., et al.* (2004). In vivo activation of the p53 pathway by small-molecule antagonists of MDM2. Science *303*, 844-848.